Theoretical Investigation of the Resonant Tunneling Phenomena and its Applications in Resonant Tunneling Diodes

Mini-project

by

René Petersen
6. Semester Nano-Physics Student
aauprojects@repetit.dk

March 23, 2007

Supervisors:
Ph.D, Thomas Garm Pedersen

Aalborg University
Faculty of Engineering and Science
Institute of Phsysics and Nanotechnology

Contents

Chapter 1

Introduction

1.1 Project Description

In this report Resonant Tunneling Diodes (RTDs) will be treated. This includes a description of the basic operational principles and a theoretical treatment of the fundemental quantum mechanical processes responsible for the operation of the device. The report will include a theoretical treatment of the following aspects:

1. Tunneling through arbitrarily formed potential barriers will be described using the transfer matrix formalism.
2. The resonant tunneling current will be calculated using the transfer matrix method.
3. Peak to valley ratios of an ideal RTD will be calculated on basis of the current calculations.
4. It will be shown that RTDs exhibit negative differential resistance in certain regions.

A program has been written in Matlab for calculation of global transmission coefficients through structures with an arbitrary number of barriers and wells and with or without an applied field. For the calculations the transfer matrix formalism has been used. Using the results of the Matlab program the current through an RTD has been calculated.

A .pdf version of this work is available at www.repetit.dk.

1.2 Tunneling Basics

Tunneling is a purely quantum mechanical phenoma which enables electrons to penetrate potential barriers even though it is classically forbidden. The scheme is illustrated in Figure 1.1. Classically the electron would be reflected if $E < V_0$ but due to tunneling there is a probability that the electron penetrates the barrier. On the other hand, clasically, if the electron has an energy $E > V_0$ it is certain to be transmitted through the barrier, but in quantum mechanics there is a probability of reflection even when the energy exceeds the barrier height.

Tunneling through a potential barrier is characterized by a transmission coefficient T so that $0 \leq T \leq 1$. The transmitted wavefunction ψ_T is thus given by $T\psi_I$ where ψ_I is the wavefunction

Figure 1.1: *The basics of tunneling. An electron of energy E is incident on a potential barrier of height V_0. Classically the electron is reflected when $E < V_0$, but quantum mechanically there is a certain probability that the electron is transmitted through the barrier.*

of the incident particle. In a single barrier structure like the one described here the transmission coefficient is a monotonically increasing function of E when $E < V_0$ ($T(E_1) > T(E_2)\ \forall\ E_1 > E_2 | V_0 > E_1$).

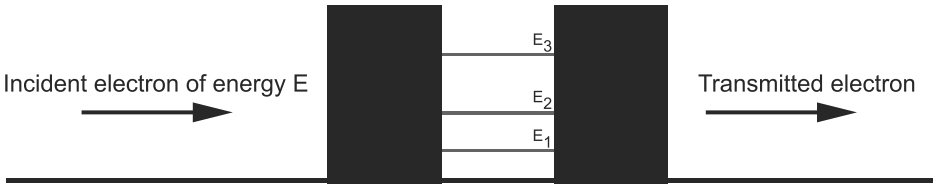

Figure 1.2: *Tunneling through a double barrier. If $T \ll 1$ for both barriers the region between the two barriers will act as a quantum well with quantized energy levels. This gives rise to resonant tunneling.*

A double barrier structure like the one shown in Figure 1.2 gives rise to a QM phenomena called resonant tunneling. If the transmission coefficients of the left and right barriers, T_L and T_R respectively, are both much smaller than unity a quantum well arises in between the barriers. This means that the energy levels in the well will be quantized. Strictly speaking this is not entirely true because T_R and T_L are in fact, of course, not equal to zero. This means that the energy levels are not clearly defined, there is some broadening of the levels. These energy levels will in the rest of the text be referred to as quasi-quantized energy levels and the bound states in the well will be referred to as quasi-bound states. When an electron with an energy which is not coincident with one of the quasi-quantized levels in the well is incident on the barrier/well complex the global transmission coefficient T_G is much smaller than unity. If however, the electron energy coincides with one of the energy levels in the well, resonance occurs and the electron can be transmitted with a transmission coefficient on the order of unity. This is the type of structure which is utilized in resonant tunneling diodes.

1.3 Resonant Tunneling Diodes and Double Barriers under Applied Voltage

Typically, in resonant tunneling diodes, the electrons come from a doped semiconductor or a metal material. The energy of the electrons can be raised by increasing the temperature or by exciting them with light, but typically it is more convenient to raise the energy by applying a voltage accross the structure. This however dramatically impacts the double barrier structure,

as is apparent from Figure 1.3. The symmetry in the system is destroyed because the two barriers no longer have the same height and therefore not the same transmission coefficient. This obviously has an impact on the energy levels in the well, and in general it will be much more difficult to obtain a global transmission coefficient $T_G \approx 1$. This effect of the applied field can be compensated for by adjusting the width of the left barrier to make it thinner than the right one, and thereby obtain equal transmission coefficients. [6].

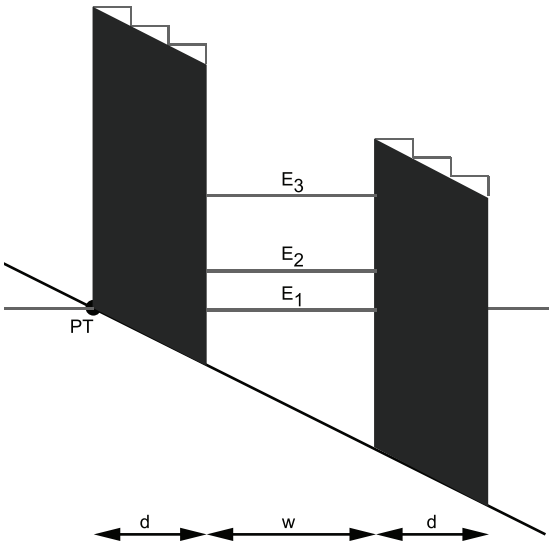

Figure 1.3: *Double barrier with an applied field. In a doped semiconductor or a metal the point marked PT will be the bottom of the conduction band, and this is from where tunneling takes place.*

One of the most interesting features of resonant tunneling diodes is the existence of a negative differential region, where the current drops when the potential increases. This is due to the nature of resonant tunneling. When the current is at a maximum the energy of the incoming electrons is equal to one of the quasi-bound states. When the potential increases further the electron energy gets more and more out of alignment with the quasi-bound states and the current drops accordingly. A typical IV-curve of an RTD is shown in Figure 1.4. When the voltage becomes high enough thermionic emission current becomes dominant and the current increases rapidly. [5]

One of the characteristics of RTDs is the peak to valley ratio. It is desirable to have the peak current as large as possible and the valley current as small as possible because this makes the negative differential resistance region more clearly defined. This relationship is expressed through the peak-to-valley ratio which should be high for a good RTD. Theoretical calculations predict ratios of as much as 1000 but in experiments this is much lower. The many experimental difficulties in producing RTDs can explain this discrepancy. Since the function of the diodes depends on quantum tunneling, the width of the barrier layers is critical. Typical widths of barrier layers are 20 Å or 40 Å [2] [8] and producing such thin layers to an adequate precision is difficult.

Another interesting feature of RTDs is their operation speed. RTDs with 712 GHz oscillation, response in the THz range and 1.5 ps switching times have been reported. The operation speed of an RTD is determind by two factors. The first one is the tunneling time which is the time

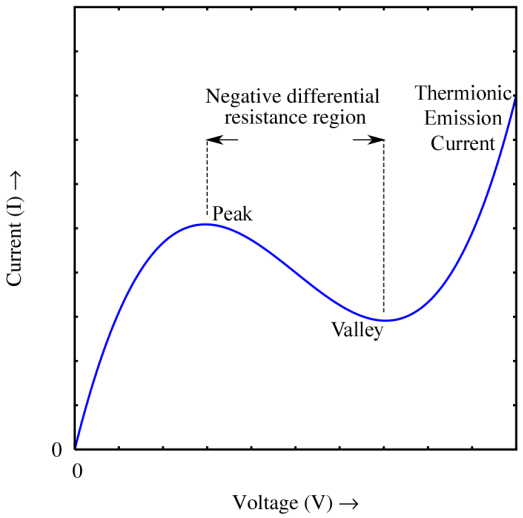

Figure 1.4: *A typical RTD IV-curve. At a certain applied voltage the current reaches a maxium, further increase of the voltage causes a decrease of current. This is the negative differential region. Increasing the voltage even further causes the current to increase rapidly due to thermionic emission.*

it takes an electron to tunnel through the barrier structure. The second factor is the time it takes to charge the RTD. The time it takes to tunnel through the barrier structure is on the order of the life time of a state in the well and this litetime is given by [3]

$$t_{life} = \frac{\hbar}{\Gamma_0} \tag{1.1}$$

where Γ_0 is the half width of the resonance peak of the energy state in question. The resonance peaks will be sharper for high and wide barriers, this means that the tunneling time can be shortened by making the barriers lower and more narrow. This however, is a tradeoff between peak-to-valley ratio and tunneling time. Usually it will not be the tunneling time but the recharge time which puts a limit to the response times of RTDs.

In the production of RTDs n-type GaAs is typically chosen as the electron donor material. The potential barriers are formed by introducing epitaxial layers of $Ga_{1-x}Ga_xAs$. Al is chosen due to its similarity to Ga. The properties of the chemical bonds they form are similar, and they have similar ion sizes. Therefore introduction of Al makes the least disturbance to the continuity of the structure and generally results in higher quality films. [2]

Chapter 2

Theory

2.1 Transfer Matrix Formalism of Quantum Tunneling

2.1.1 Constant Potential

In this section the transfer matrix formulation of quantum tunneling will be described and the results derived [3] [1]. To describe the technique the simple scenario in Figure 2.1 will be considered.

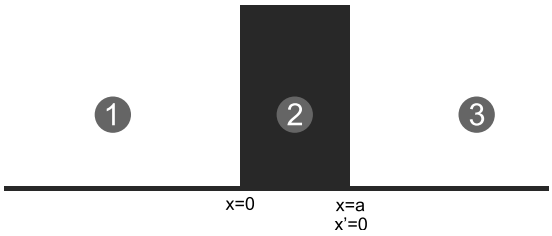

Figure 2.1: *Tunneling through a single barrier.*

In region 1 the wave function is termed ψ_1 and the potential is zero, in region 2 the wave function is termed ψ_2 and the potential is V_0 and in region 3 the wave function is termed ψ_3 and the potential is again zero. The solutions to the Schrödinger equation in these three regions are

$$\psi_1 = Ae^{ik_1x} + Be^{-ik_1x} \tag{2.1}$$
$$\psi_2 = Ce^{ik_2x} + De^{-ik_2x} \tag{2.2}$$
$$\psi_3 = Fe^{ik_3x} + Ge^{-ik_3x} \tag{2.3}$$
$$\tag{2.4}$$

where $k_i = \sqrt{2m\left(E - V_i\right)}$. The wave function and its derivative is required to be continous at the discontinuity between adjacent regions, ie. at $x = 0$ and $x = a$. This requirement is imposed in order to avoid abrubt changes in probability density. Using these two continuity conditions between region 1 and 2 yields the two equations

$$\psi_1(0) = \psi_2(0) \quad \text{and} \quad \frac{d\psi_1}{dx}\Big|_{x=0} = \frac{d\psi_2}{dx}\Big|_{x=0} \tag{2.5}$$

Which gives the following restrictions on the coefficients

$$\begin{aligned} A + B &= C + D & (2.6)\\ ik_1A - ik_1B &= ik_2C - ik_2D & (2.7) \end{aligned}$$

These conditions can be written in matrix form

$$\begin{pmatrix} 1 & 1 \\ ik_1 & -ik_1 \end{pmatrix} \cdot \begin{pmatrix} A \\ B \end{pmatrix} = \begin{pmatrix} 1 & 1 \\ ik_2 & -ik_2 \end{pmatrix} \cdot \begin{pmatrix} C \\ D \end{pmatrix} \tag{2.8}$$

Using the inverse matrix theorem an expression connecting coefficients (A, B) with (C, D) can be obtained

$$\begin{pmatrix} A \\ B \end{pmatrix} = \frac{1}{2} \begin{pmatrix} 1 + \frac{k_2}{k_1} & 1 - \frac{k_2}{k_1} \\ 1 - \frac{k_2}{k_1} & 1 + \frac{k_2}{k_1} \end{pmatrix} \cdot \begin{pmatrix} C \\ D \end{pmatrix} = \mathbf{M_{12}} \cdot \begin{pmatrix} C \\ D \end{pmatrix} \tag{2.9}$$

The matrix $\mathbf{M_{12}}$ is known as the discontinuity matrix and it connects the wave function in region 1 with the wave function in region 2, ie. it describes the propagation of the wave function across a boundary.

The wave function is also required to be continous across the boundary between region 2 and region 3. A new coordinate system (coordinates in this new system are marked with a prime) is chosen so that $x' = 0$ at $x = a$ and the primed coordinate system is therefore related to the unprimed one by $x' = x - a$. The continuity conditions are then

$$\psi_2'(0) = \psi_3'(0) \quad \text{and} \quad \frac{d\psi_2'}{dx'}\Big|_{x'=0} = \frac{d\psi_3'}{dx'}\Big|_{x'=0} \tag{2.10}$$

where ψ_2' and ψ_3' are the wave functions in the new primed coordinate systems. These conditions yields a matrix similar to $\mathbf{M_{12}}$ in Equation 2.9. To obtain a connection between the primed wave function and the unprimed one the relation $\psi_2(x) = \psi_2'(x - a)$ is exploited

$$Ce^{ik_2x} + De^{-ik_2x} = C'e^{ik_2(x-a)} + D'e^{-ik_2(x-a)} \tag{2.11}$$

Or, written in matrix form

$$\begin{pmatrix} e^{ik_2x} & e^{-ik_2x} \end{pmatrix} \cdot \begin{pmatrix} C \\ D \end{pmatrix} = \begin{pmatrix} e^{ik_2x} & e^{-ik_2x} \end{pmatrix} \cdot \begin{pmatrix} C'e^{-ik_2a} \\ D'e^{ik_2a} \end{pmatrix} \cdot \tag{2.12}$$

Cancelling the row vector it is seen that the relation between the primed and unprimed coordinates is described by

$$\begin{pmatrix} C \\ D \end{pmatrix} = \begin{pmatrix} e^{-ik_2 a} & 0 \\ 0 & e^{ik_2 a} \end{pmatrix} \cdot \begin{pmatrix} C' \\ D' \end{pmatrix} = \mathbf{M_P} \cdot \begin{pmatrix} C' \\ D' \end{pmatrix} \tag{2.13}$$

where $\mathbf{M_P}$ is called the propagation matrix. It describes the propagation of the wave function between two boundaries and a is the distance between the points to be connected. In the case considered here it describes the propagation of the wave function inside the barrier. When inside a barrier the k_i's are purely imaginary and the matrix becomes an operator scaling the operand by an exponentially decaying factor, which is the behaviour expected from a matrix describing propagation within a potential barrier. The matrix $\mathbf{M_P}$ can equally well be used to describe propagation inside a quantum well, in which case it modulates the operand by a plane wave, ie. it is a phase-shift operator .

As an example consider a situation like the one depicted in Figure 1.2. The left region of zero potential is labelled 1, the left barrier 2, the zero potential well 3, the right barrier 4 and the right region of zero potential 5. The system matrix (the matrix describing propagation through the whole system from 1 to 5) is then given by

$$\mathbf{M_S} = \mathbf{M_{12}} \cdot \mathbf{M_B} \cdot \mathbf{M_{23}} \cdot \mathbf{M_W} \cdot \mathbf{M_{34}} \cdot \mathbf{M_B} \cdot \mathbf{M_{45}} \tag{2.14}$$

The coefficients (A,B) are therefore related to the coefficients (F,G) by

$$\begin{pmatrix} A \\ B \end{pmatrix} = \mathbf{M_S} \cdot \begin{pmatrix} F \\ G \end{pmatrix} \tag{2.15}$$

The transmission coefficient of a barrier is equal to the square of the transmitted wave, divided by the square of the incoming wave. Setting G equal to zero because there is no incoming wave in region 5 the transmission coefficient through the whole system can be expressed as

$$T = \frac{|Fe^{ik_1 x}|^2}{|Ae^{ik_5 x}|^2} = \frac{F^* F}{A^* A} \tag{2.16}$$

where * denotes complex conjugate. From Equation 2.15 it is seen that $A = M_{S,11} F$ (G is zero), therefore

$$T = \frac{F^* F}{(M_{S,11} F)^* (M_{S,11} F)} = \frac{1}{M^*_{S,11} M_{S,11}} = \frac{1}{|M_{S,11}|^2} \tag{2.17}$$

2.1.2 Arbitrary Potential

In the last section the potential considered was of rectangular shape. In this section the results will be generalized to potentials of arbitrary shape. The generalization is not very difficult,

the arbitrary potential is divided into a number of square potential barrier divisions of width d and separated by quantum wells of width w. The system matrix is then calculated in the limit when w goes to zero, corresponding to the barriers being infinitely close together (no quantum well between them). The matrix of an abritrary barrier can then be calculated by

$$\mathbf{M_S} = \mathbf{M_{12}} \cdot \mathbf{M_{B2}} \cdot \mathbf{M_{23}} \cdot \mathbf{M_{W3}} \cdot \mathbf{M_{34}} \cdot \mathbf{M_{B4}} \cdot \mathbf{M_{45}} ... \tag{2.18}$$

where M_S denotes the system matrix, ie. the matrix describing the propagation of the wave function through the whole system of barriers and wells. When the well depth goes to zero the $\mathbf{M_{Wx}}$ matrices become unit matrices, as is clearly seen from Equation 2.13. This leaves behind the expression

$$\mathbf{M_S} = \mathbf{M_{12}} \cdot \mathbf{M_{B2}} \cdot \mathbf{M_{23}} \cdot \mathbf{M_{34}} \cdot \mathbf{M_{B4}} \cdot \mathbf{M_{45}} ... \tag{2.19}$$

The product of the two matrices $\mathbf{M_{23}M_{34}}$ is a product of two propagation matrices (Equation 2.9). Multiplying the two matrices gives the matrix

$$\mathbf{M_{24}} = \mathbf{M_{23}} \cdot \mathbf{M_{34}} = \frac{1}{2k_2} \begin{pmatrix} k_2 + k_4 & k_2 - k_4 \\ k_2 - k_4 & k_2 + k_4 \end{pmatrix} \tag{2.20}$$

Taking the limit when d (the barrier division width) goes to zero would produce an infinite number of matrices so a finite width has to be chosen. The number of square barriers to divide each arbitrary barrier into to obtain correct results depend on the arbitraryness of the barrier. A parabolic shaped potential requires more divisions than a barrier where one side is at only a sligthly lower potential than the other side to get valid results. Generally, in situations where the barriers change rapidly more barrier divisions are required to obtain correct results. In the transfer matrix method no approximations have been made, this means that the accuracy is determined solely by the number of divisions into which arbitrary potentials are divided.

2.2 Current in a Resonant Tunneling Diode

To calculate the tunneling current through the multibarrier complex it is necessary to consider the Fermi distributions in the semiconductor or metal structures surrounding the barriers. The Fermi distributions give the probability that an electron state of a certain energy is occupied. If the Fermi distribution on the left hand side is termed f_L and the distribution on the right hand side f_R the tunneling current is proportional to

$$I \propto \int_0^\infty T(E) \left[f_L(E) - f_R(E) \right] D(E) dE \tag{2.21}$$

where $D(E)$ is the density of states (DOS) and $T(E)$ is the probability of tunneling for an electron of energy E. For an electron to travel through the barrier complex there has to be an electron with an appropriate energy in the electron donor material and an unoccopied electron

level for this electron in the acceptor material. This behaviour is taken care of by the term in the sharp parentheses. When $f_L(E) = 1$ and $f_R(E) = 0$ an electron can travel from left to right. When $f_L(E)$ and $f_R(E)$ are both zero or both unity the electron with energy E does not contribute to the total current. The Fermi distributions for the left and right hand sides are given by

$$f_L(E) = \frac{1}{e^{(E+eV-E_F)/kT}+1} \quad \text{and} \quad f_R(E) = \frac{1}{e^{(E-E_F)/kT}+1} \tag{2.22}$$

where E_F is the fermi energy under zero applied field. Electrons in the left hand side will have an energy which differs from the zero field case by $-eV$. Assuming that a potential $V < 0$ is applied to the left metal (the right metal being grounded), the electrons are raised to higher energy levels and the fermi energy increases accordingly. This means that the fermi energy will be higher in the left metal than in the right one, thus the difference between the fermi distributions on the left and right. The density of states $D(E)$ for a free electron Fermi gas in three dimensions is given by

$$D(E) = \frac{\sqrt{2}m_e^{3/2}}{\pi^2\hbar^3}\sqrt{E-E_C}\theta(E-E_C) \tag{2.23}$$

where E_C is the energy of the conduction band bottom and $\theta(E-E_C)$ is the heaviside step function. When the energy E is lower than the conduction band edge the density of states is zero. If all energies are measured relative to the conduction band bottom the DOS expression reduce to

$$D(E) = \frac{\sqrt{2}m_e^{3/2}}{\pi^2\hbar^3}\sqrt{E} \tag{2.24}$$

Inserting this in the expression for the current gives

$$I \propto \int_0^\infty T(E)\left[f_L(E) - f_R(E)\right]\sqrt{E}dE \tag{2.25}$$

Where the constants from the DOS expression have been omitted because they make no difference for the proportionality.

Chapter 3

Calculations and Discussion

3.1 Method of Calculation

To calculate the tunneling probabilities through the barrier complex the method described in Section 2.1 is used. The barriers and the wells are in all applied field calculations divided into 30 divisions, which should be enough when the barriers and wells are simply trapezoid. Had the barriers been of a more complicated shape a higher number of divisions would be needed. Generally the number of divisions necessary depends on how rapidly the barrier shape varies with position. The following calculations are made

1. Transmission and current calculations of double and triple and five barrier structures with no applied field
2. Transmission and current calculations of double and triple barrier structures under an applied field
3. Current calculations of a double barrier structure with a 100 Å well to investigate the influence of well width on the number of quasi bound states

In all cases, except for number 3 where the barrier width was set to 100 Å, the barriers were of width 20 Å, the wells were of width 50 Å and the barrier height was 0.5 eV as in [8]. All graphs are plotted on a logarithmic scale. The electron effective mass used was $0.066m_e$ [4].

As described in the theory chapter the current can be calculated from Equation 2.25. Since there is no analytical expression for $T(E)$ the integration will have to be carried out numerically.

The piece of Matlab code responsible for calculation of transmission coefficient is the most central part of the code. The code can be found in Appendix A.

3.2 T_G and Current Calculations with no Applied Field

In this section the calculations of transmission coefficient under zero applied field are presented. The calculations are made for double, triple and five barrier structures. The graphs have been made by dividing the interval 0.05 eV to 0.6 eV into 100000 points. This should be enough to get all the details of the spectrum even though the resonance peaks are very sharp.

In Figure 3.1 the transmission coefficient (T_G) plots under zero applied field are shown. No interesting details are seen above 0.6 eV where the transmission coefficient becomes very close to unity for all energies. This is because the barrier height was set to 0.5 eV and energies higher than this will produce transmission coefficients on the order of unity.

The immediately apparent difference between the three plots is the splitting of the peaks into several closely spaced peaks when more barriers are added. The number of closely spaced peaks equals the number of barriers minus one.

In the double barrier case the peaks are located where true bound eigenstates would be located if the quantum well was infinitely wide. In the triple and five-barrier cases it would thus seem like the presence of additional barriers results in additional bound eigenstates in the well.

Comparing these calculations with fig. 2 of reference [8] it is seen that the peaks are generally shifted to lower energies. This could be explained by differences in the effective mass of electrons used.

From the graphs it is seen that the energy of the first quasi bound state is around 0.1 eV. GaAs has a fermi energy $E_f \approx 0.005eV$ for a doping of $n = 10^{17}cm^{-}3$ [8]. This means that none of the mobile electrons have energies large enough to reach one of the quasi bound states, unless the temperature is high. To increase the fermi energy a potential difference is imposed across the structure. Calculations of the current under these conditions is described in the next section.

3.3 Current Calculations under an Applied Voltage

When a potential difference is imposed on the barrier structure a current flows. In this section graphs showing the current and transmission coefficient as a function of applied potentials are presented. The graphs was made using the theory described in Section 2.1.2 and Section 2.2. As briefly stated earlier in this chapter, the integration for current calculations will have to be carried out numerically since no analytical expression for the transmission coefficient is obtained when using the transfer matrix formalism. To obtain the graphs the transmission coefficients was calculated for energies between 0 and E_F using 100000 points in the interval, this was done for potentials between 0 and 2 V using 250 points in this interval. The temperature is taken to 0 kelvin, which means that no states above the fermi level will be occupied, therefore it is enough to perform the integration from 0 eV and up to the fermi energy. The calculated currents are in arbitrary units, therefore the graphs does not give any information about the actual current but only the current maxima and minima. In the calculations it is assumed that the potential drops linearly over the entire structure. In reality however, the potential will not drop uniformly over the structure due to differences in the layer materials.

In Figure 3.2 the tunneling probability in a double barrier structure under an applied voltage between 0 V and 0.3 V is shown. Comparing this graph to Figure 3.1(a) the important result that T_G does not become unity when resonance occurs under applied voltage is apparent. This is due to the asymmetry of the barriers due to the applied voltage. When a voltage is applied the barriers no longer have the same height for an electron of energy E. This also means that they will no longer have the same transmission coefficient and this makes it much harder to obtain global transmission coefficients of 1. The difference in transmission coefficient of the two barriers can be compensated for by adjusting the width of one of the barriers. This optimization can only be done for one particular peak though.

In Figure 3.3 the current is calculated as a function of applied voltage in a double barrier

structure. The important feature to note in this figure is that the current is peaked at a certain voltage. This is where resonant tunneling appears. The region that follows is where the negative differential resistance occurs, the current drops when the applied voltage increases. The negative differential resistance region is where the fermi level crosses the energy of one of the quasi-bound states in the well.

The peak-to-valley ratio is seen to be about 1000, which is very high compared to the experimentally obtained values. In [7] peak-to-valley ratios of 7.6 has been obtained using triple barrier structures, which is far less than the theoretical calculations predict. This discrepancy is explanied by the experimental difficulties in producing RTDs and the fact that resonant tunneling is strongly dependent on experimental parameters.

In the current plot only one resonance peak is present, but genereally the number of resonance peaks is dependent on the width of the well region between the barriers. The spacing between the energy levels in a quantum well is proportional to $1/w^2$ where w is the width of the well. Therefore the number of peaks should increase when well width is inreased. This is shown in Figure 3.4 where the well width is set to 100 Å. It is also apparent from the graph that the energy of the lowest lying quasi bound state is shifted towards lower energies. This is also to be expected because the energy levels are also proportional to $1/w^2$.

In Figure 3.5 the current is plotted as a function of applied voltage in triple barrier structure. From these graphs it is seen that three peaks are present as opposed to the double barrier plot in Figure 3.3 where only two peaks are present.

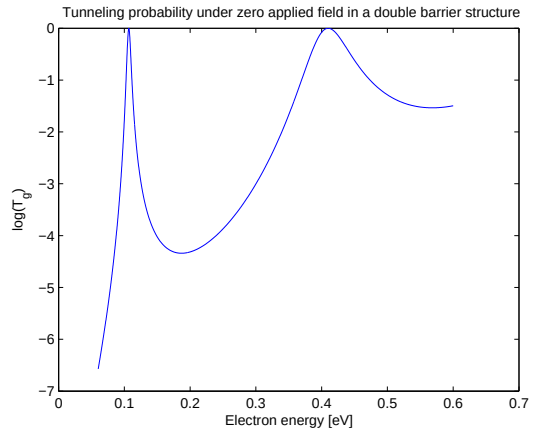

(a)

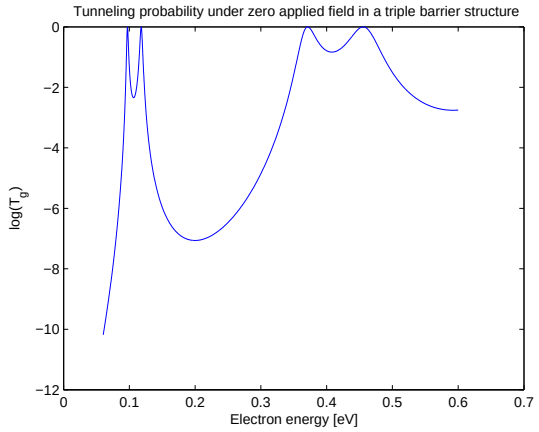

(b)

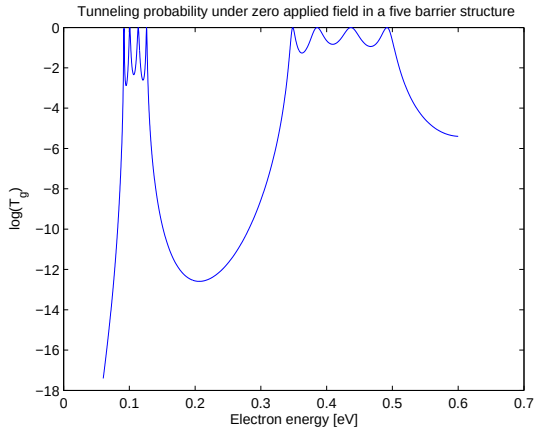

(c)

Figure 3.1: *The transmission coefficient calculations under zero applied field. It is seen that the peaks are split when more barriers are added.*

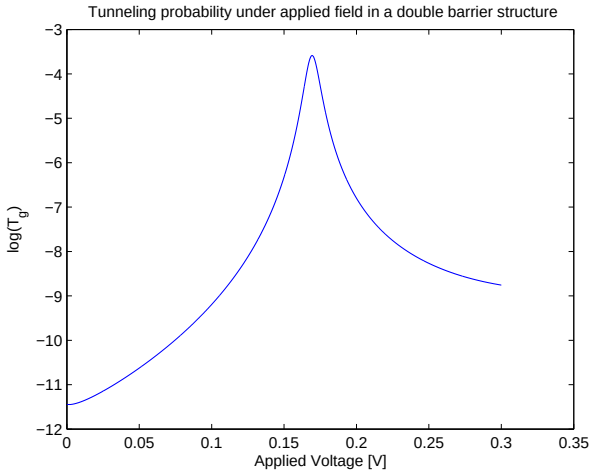

Figure 3.2: *Tunneling probability under an applied voltage between 0 V and 0.3 V in a double barrier structure. The important feature to note is that the tunneling probability does not become unity when resonance occurs.*

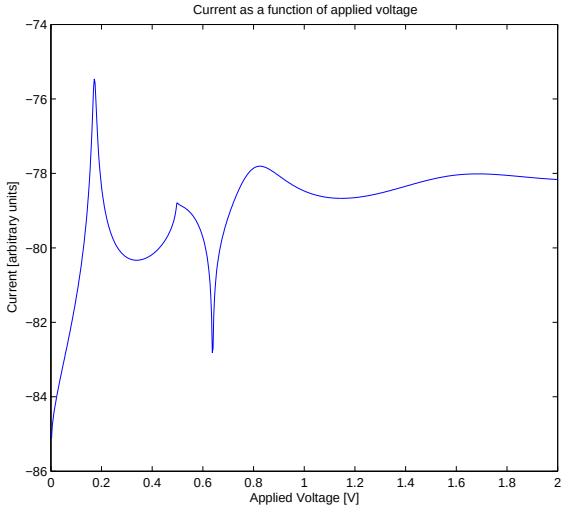

Figure 3.3: *The tunneling current in a double barrier structure under an applied voltage of 0 V to 2 V. The large peak is due to resonant tunneling. The negative differential resistance region is the region following the peak where the current drops as a function of applied voltage.*

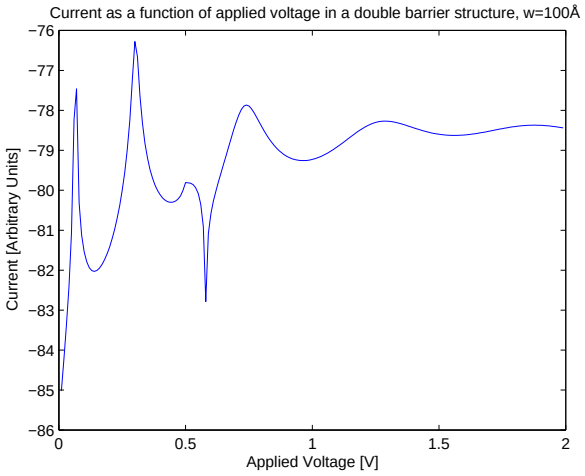

Figure 3.4: *The tunneling current in a double barrier structure under an applied voltage of 0 V to 2 V width a well width of 100 Å. It is seen that two clear peaks appear when the well width is increased.*

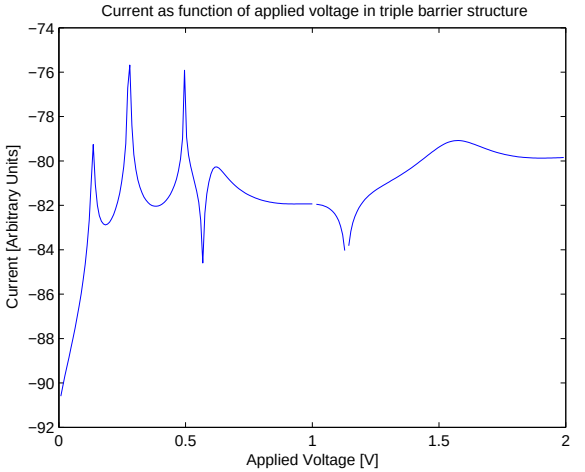

Figure 3.5: *The tunneling current in a triple barrier structure under an applied field of 0 V to 2 V. The large peaks are due to resonant tunneling. Two regions of negative differential resistance are seen.*

Chapter 4

Conclusion

The theory of tunneling using the transfer matrix formalism has been investigated. The theory has been applied to resonant tunneling diodes and used to calculate the current through such a device under an applied voltage. It can be concluded that tunneling through symmetric double, triple or five-barrier structures can reach T_G values of 1 when resonance occurs. In triple and five-barrier structures the resonance peaks are split into several small peaks where the number of small peaks is generally equal to $(n-1)$. It can also be concluded that in asymmetric barrier structures it will in general be much harder to obatin T_G values of 1.

From the calculations it is seen that a region of negative differential resistance in resonant tunneling diodes exists. The calculations predict peak-to-valley ratios of 1000 which is much more than in experiments. This discrepancy must be ascribed to the ideal nature of the theoretical model.

Appendix A

Matlab Program

In this appendix the code to the piece of Matlab code responsible for calculation of global transmission coefficients is shown.

```
function Transmission = rtTransmission(AV, En, Prec)

AA=10^-10;
eV=1.602*10^-19;
me=0.066*9.109*10^-31;
hbar=6.626*10^-34 / (2*pi);
q=1.602*10^-19; % electron charge

Energy=En+AV*q;      % energy of the tunneling electron in eV

% this vector contains widths of all barriers and wells in the system. When
% n is odd it is a barrier, when n is even it is a well
Widths=[20.0*AA, 50.0*AA, 20.0*AA, 50.00*AA,
            20.00*AA, 50.0*AA, 20.0*AA, 50.00*AA, 20.00*AA];

% can only be an odd number, obviously, because we cannot have a
% barrier-well construct without a right barrier.
Entries=3;

% the width of the whole barrier/well construct
xmax=0;
for n=1:Entries
    xmax = xmax + Widths(n);
end
```

```
% the slope of the system, potential drop per Ångstroem,
% this depends on the applied field
Slope = AV*eV / xmax;

% potentials vector, case of no applied field, odd n is barrier, even is a
% well.
Pots=[0.5*eV, 0.0*eV, 0.5*eV, 0.0*eV, 0.5*eV, 0.0*eV, 0.5*eV, 0.0*eV, 0.5*eV];
Pot0Left=AV*q;  % Potential outside the barrier/well construct to the left
Pot0Right=0*eV; % Potential to outside the barrier/well construct to the right
Precision=Prec;    % number of square wells to divide each barrier into

% moving in
kr = sqrt( 2*me*(Pots(1) + Pot0Left - Energy) ) / hbar;
kl = sqrt( 2*me*(Energy - Pot0Left))/hbar;
SysMat(1,1)=1-i*kr/kl;      SysMat(1,2)=1+i*kr/kl;
SysMat(2,1)=1+i*kr/kl;      SysMat(2,2)=1-i*kr/kl;
SysMat=0.5*SysMat;

% loop of the whole system
for n=1:Entries

    xposl = 0;
```

```
    for j=1:(n-1)
        xposl = xposl + Widths(j);
    end
    DivW = Widths(n)/Precision; % width of a single division

    % Potential at left side of barrier division
    potl = Pots(n) + AV*q - xposl*Slope;

    % single barrier/well loop, this loop divides a single barrier into several
    % square barriers/wells and multiplies the matrices together
    for l=1:Precision

        % the xposr variable allows us to determine the potential on the
        % right side of this barrier division
        potr = potl - DivW*Slope;

        % setup the matrix of this division. for even n it is a well, for
        % odd n it is a barrier
        if( mod(n,2) == 1 ) % odd n, barrier
            a = sqrt(2*me*(potl - Energy))/hbar;
            M(1,1) = exp(-a*DivW); M(1,2) =          0;
            M(2,1) =          0; M(2,2) =  exp(a*DivW);
        else % even n, well
            k = sqrt(2*me*(Energy - potl))/hbar;
            M(1,1) = exp(-i*k*DivW); M(1,2) =          0;
            M(2,1) =          0; M(2,2) =  exp(i*k*DivW);
        end
        SysMat=M*SysMat;

        % setup matrix for crossing the discontinuity between two barrier or well
        % divisions. Only do this when we are inside a barrier or a well, when
        % we get out of the right side of it, we have to multiply by a discontinuity
        % matrix from a well to a barrier instead.
        if(l<Precision)
            if( mod(n,2) == 1 ) % odd n, we are in a barrier
                k1= sqrt(2*me*(potr - Energy))/hbar; % right
                k2= sqrt(2*me*(potl - Energy))/hbar; % left
            else % even n, we are in a well
                k1= sqrt(2*me*(Energy - potr))/hbar; % right
                k2= sqrt(2*me*(Energy - potl))/hbar; % left
            end

            M(1,1) = k2+k1; M(1,2) = k2-k1;
            M(2,1) = k2-k1; M(2,2) = k2+k1;
            SysMat = (0.5*M*SysMat)/k2;

            potl = potr;
        end
    end % single barrier/well loop

    % check if we are still inside the system, or if we are moving out of
    % the rightmost barrier
    if n < Entries
        if( mod(n,2) == 1 ) % barrier to well
            a = sqrt( 2*me*(potl - Energy))/hbar;
            k = sqrt( 2*me*(Energy - Pots(n+1)))/hbar;
            M(1,1) = 1+i*k/a; M(1,2) = 1-i*k/a;
            M(2,1) = 1-i*k/a; M(2,2) = 1+i*k/a;
        else % well to barrier
            a = sqrt( 2*me*(Pots(n+1) - Energy))/hbar;
            k = sqrt( 2*me*(Energy - potl))/hbar;
            M(1,1) = 1-i*a/k; M(1,2) = 1+i*a/k;
            M(2,1) = 1+i*a/k; M(2,2) = 1-i*a/k;
        end
        SysMat = 0.5*M*SysMat;
    else % moving out, last thing to do
        kl = sqrt( 2*me*( potl - Energy ) ) / hbar;
        kr = sqrt(2*me*(Energy - Pot0Right))/hbar;
        M(1,1)=1+i*kr/kl;    M(1,2)=1-i*kr/kl;
        M(2,1)=1-i*kr/kl;    M(2,2)=1+i*kr/kl;
        SysMat=0.5*M*SysMat;
        Transmission = 1/abs(SysMat(1,1))^2;
    end
end % barrier loop
```

Bibliography

[1] The transfer matrix method. `http://www.iljinnanotech.co.kr/en/home.html`.

[2] L. L. Chang, L. Esaki, and R. Tsu. Resonant tunneling in semiconductor double barriers. *Applied Physics Letters*, 24, 1974.

[3] Koichi Meazawa and Arno Förster. *Nanoelectronics and Information Technology*. Wiley, 2003.

[4] T. G. Pedersen and L. Diekhöner. *Electrical, optical and magnetic properties of nanostructures*. Aalborg University, 2007.

[5] Mohsen Razavy. *Quantum Theory of Tunneling*. World Scientific Publishing Company, 2003.

[6] B. Ricco and M. Ya. Azbel. Physics of resonant tunneling. the one-dimensional double-barrier case. *Physical Review B*, 22, 1983.

[7] Yoshiyuki Suda and Hajime Koyama. Electron resonant tunneling with a high peak-to-valley ratio at room temperature in $si_{1-x}ge_x/si$ triple barrier diodes. *Applied Physics Letters*, 79, 2001.

[8] R. Tsu and L. Esaki. Tunneling in a finite superlattice. *Applied Physics Letters*, 22, 1973.